

# Supporting Information

Stevenson, S.<sup>1</sup>, Deser, C.<sup>2</sup>, Coats, S.<sup>3</sup>, Falster, G.<sup>4</sup>, Konecky, B.<sup>5</sup>, Maher, N.<sup>4</sup>,

Pfleger, C<sup>1</sup>.

<sup>1</sup>Bren School of Environmental Science and Management, University of California, Santa Barbara, Santa Barbara, CA, USA

<sup>2</sup>National Center for Atmospheric Research, Boulder, CO, USA

<sup>3</sup>University of Hawaii at Manoa, Honolulu, HI, USA

<sup>4</sup>Australian National University, Canberra, ACT, Australia

<sup>5</sup>Washington University of St Louis, St. Louis, MO, USA

## Contents of this file

1. Tables S1 to S3
2. Figures S1 to S5

## 1. Figures and Tables

---



**Table S1.** SMILE temperature datasets used in the present analysis. Numbers indicate the ensemble size associated with each set of external forcing factors. <sup>a</sup>*EC-Earth: SSP5-8.5 data used only for members corresponding to a historical simulation*

Model name	Historical	SSP5-8.5	SSP3-7.0	SSP2-4.5	SSP1-2.6
ACCESS-ESM1-5	40	40	40	40	40
CanESM5	40	25	25	25	25
CESM2	100	15	100	16	
E3SMv1	20		20		
E3SMv2	20		20		
EC-Earth3 <sup>a</sup>	25	15			
GFDL-SPEAR	30	30			
IPSL-CM6A-LR	33	7	11		
MIROC6	50	50	3	50	50
MIROC-ES2L	30	10	10		

**Table S2.** Equatorial SST gradient sensitivity for all models considered in the present analysis. Epoch difference is calculated between 1950-2000 and 2050-2100; all values have been normalized to the global-mean temperature epoch difference. Units are C/C. Data from all calendar months is used for all calculations. “Uncertainty” indicates the difference between the maximum and minimum sensitivity estimates, generated for each available emissions scenario. A value of N/A for this parameter indicates that only a single emissions scenario was available for that model.

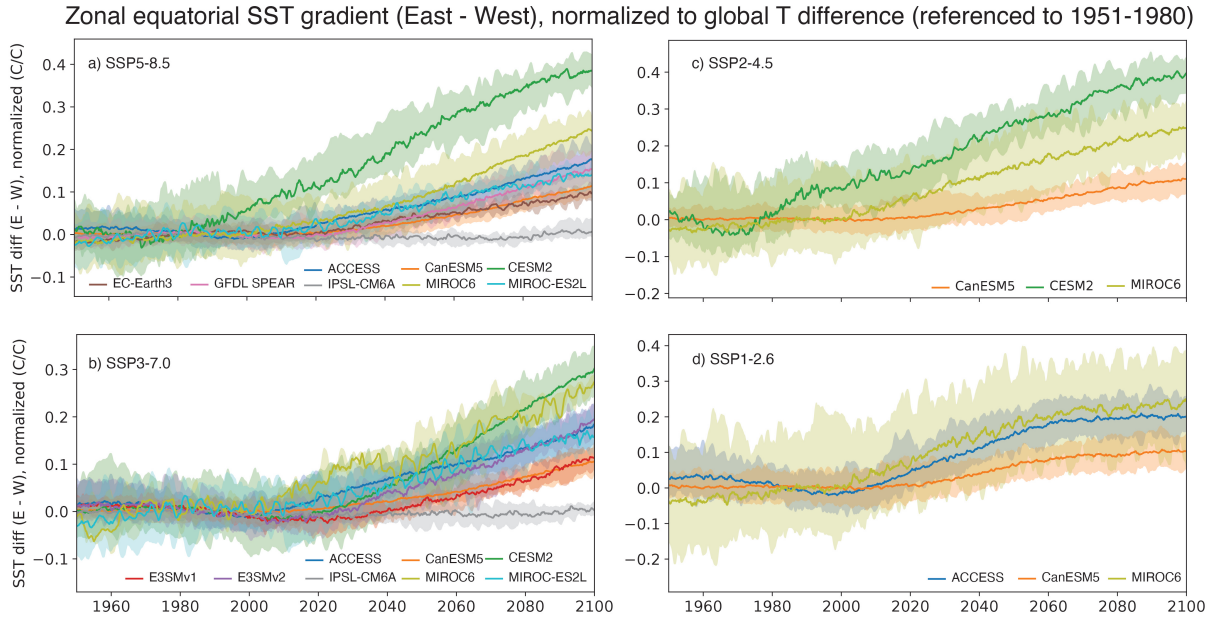
Model name	Sensitivity	Uncertainty
ACCESS	0.126	0.052
CanESM5	0.058	0.014
CESM2	0.308	0.12
E3SMv1	0.108	N/A
E3SMv2	0.157	N/A
EC-Earth3	0.0437	N/A
GFDL-SPEAR	0.148	N/A
IPSL-CM6A	0.0743	0.008
MIROC6	0.262	0.044
MIROC-ES2L	0.182	0.022

**Table S3.** Same as Table S2, but using linear trend estimates over 1950-2100 calculated using the ensemble mean. Units of trend are C/decade/C.

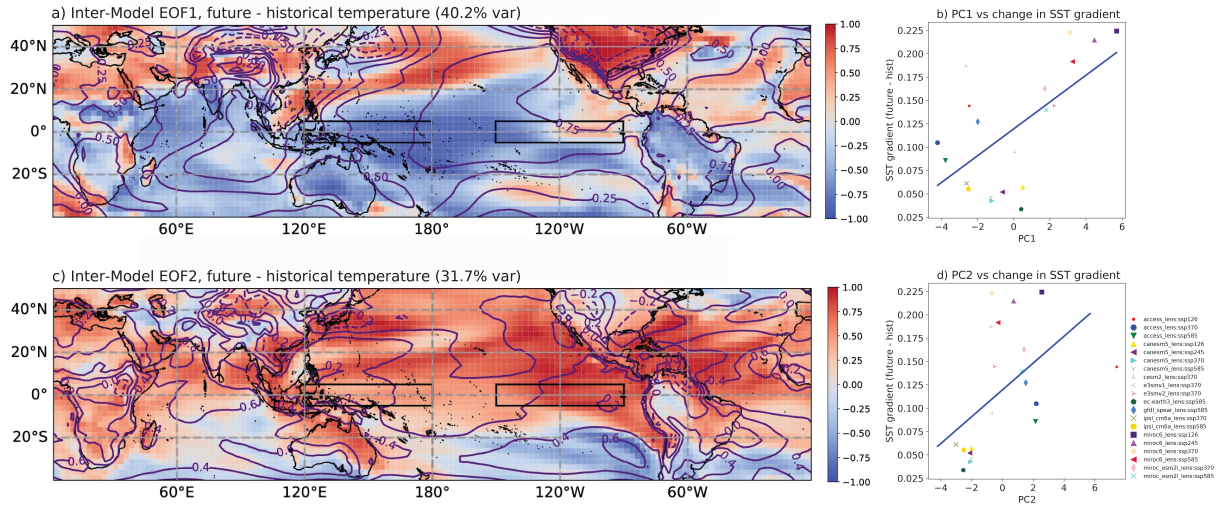
Model name	Trend	Uncertainty
ACCESS	0.0148	0.0034
CanESM5	0.00844	0.00056
CESM2	0.0292	0.0095
E3SMv1	0.00812	N/A
E3SMv2	0.0145	N/A
EC-Earth3	0.0081	N/A
GFDL-SPEAR	0.012	N/A
IPSL-CM6A	$-7.32 \times 10^{-5}$	0.00031
MIROC6	0.020	0.0028
MIROC-ES2L	0.0126	0.0017

**Table S4.** List of ensembles which are members of the different model groupings mentioned in the main text: ‘high-sensitivity’, ‘low-sensitivity’, ‘wet’, and ‘dry’. Group membership is indicated by an X in the relevant column for each model.

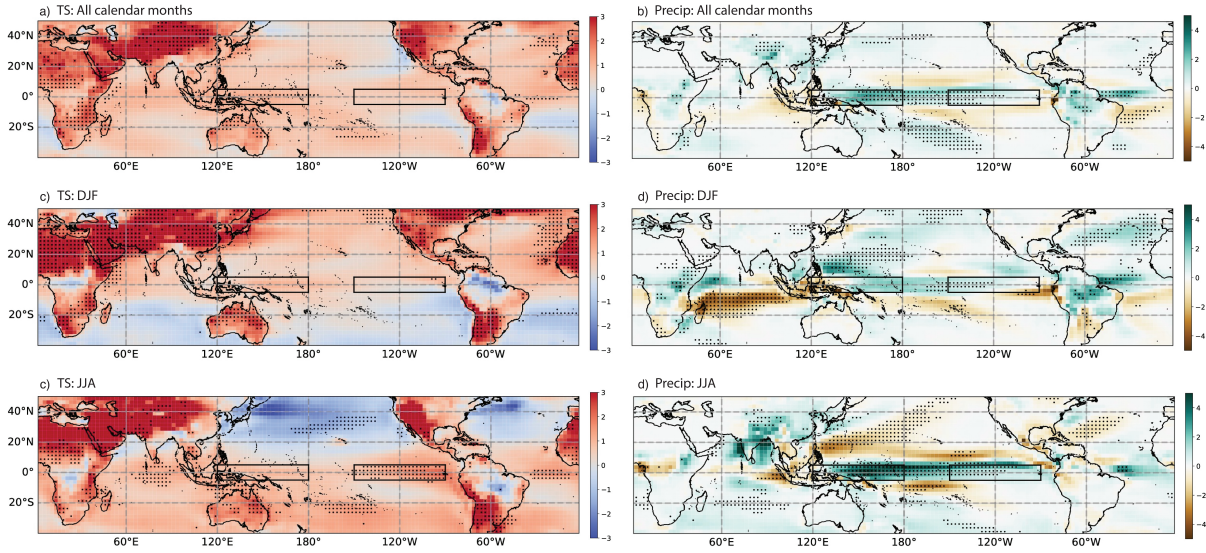
Model name	High-Sens.	Low-Sens.	Wet	Dry
ACCESS	X			X
CanESM5		X		X
CESM2	X		X	
E3SMv1		X		X
E3SMv2	X		X	
EC-Earth3		X		X
GFDL-SPEAR				X
IPSL-CM6A		X		X
MIROC6	X		X	
MIROC-ES2L			X	



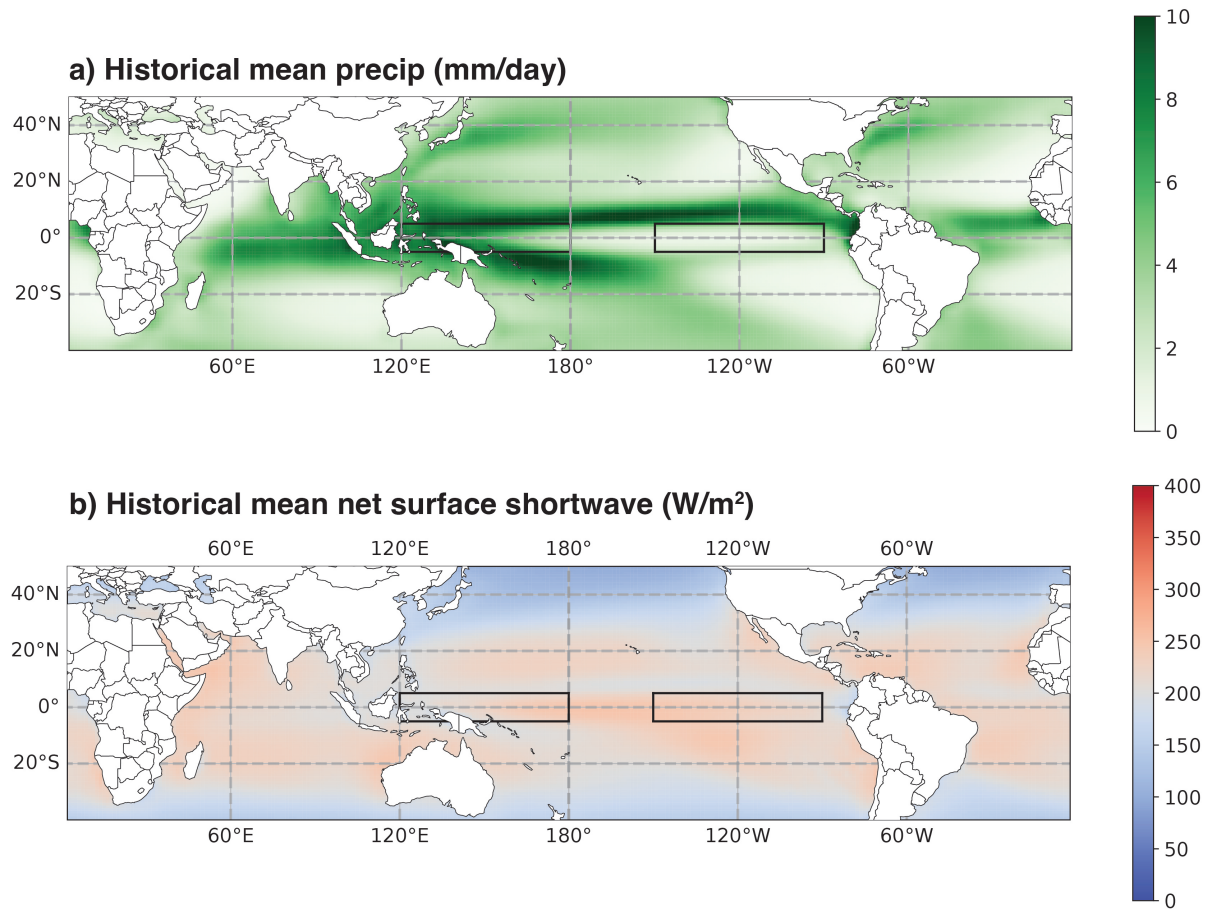
**Figure S1.** Running 30-year mean zonal SST gradient time series for SMILEs run under different emissions scenarios: a) SSP5-8.5; b) SSP3-7.0; c) SSP2-4.5; d) SSP1-2.6. All SST gradient time series have been normalized to the ensemble-mean global temperature change between 2050-2099 and 1951-1999 prior to plotting. Solid lines indicate the ensemble median, and shaded envelopes the ensemble min/max. The normalized zonal SST gradient difference between the 1951-1990 reference period has been subtracted from all time series to ensure overlap between ensembles.



**Figure S2.** Spatial patterns of correlations of temperature (colors) and sea level pressure (contours) with the first two principal components of ensemble-mean temperature difference, calculated between 2050-2099 and 1950-1999. Here the ensemble mean temporal differences in each model/scenario combination are treated as individual data points (see also legend next to panel d), and the EOFs are computed along the [model+scenario] dimension, as discussed in the main text. a) Spatial pattern of Mode 1; b) PC1 versus the future - historical difference in the SST gradient; c) Spatial pattern of Mode 2 ( $R^2 = 0.38$ ); d) PC2 versus future - historical SST gradient difference ( $R^2 = 0.28$ ).

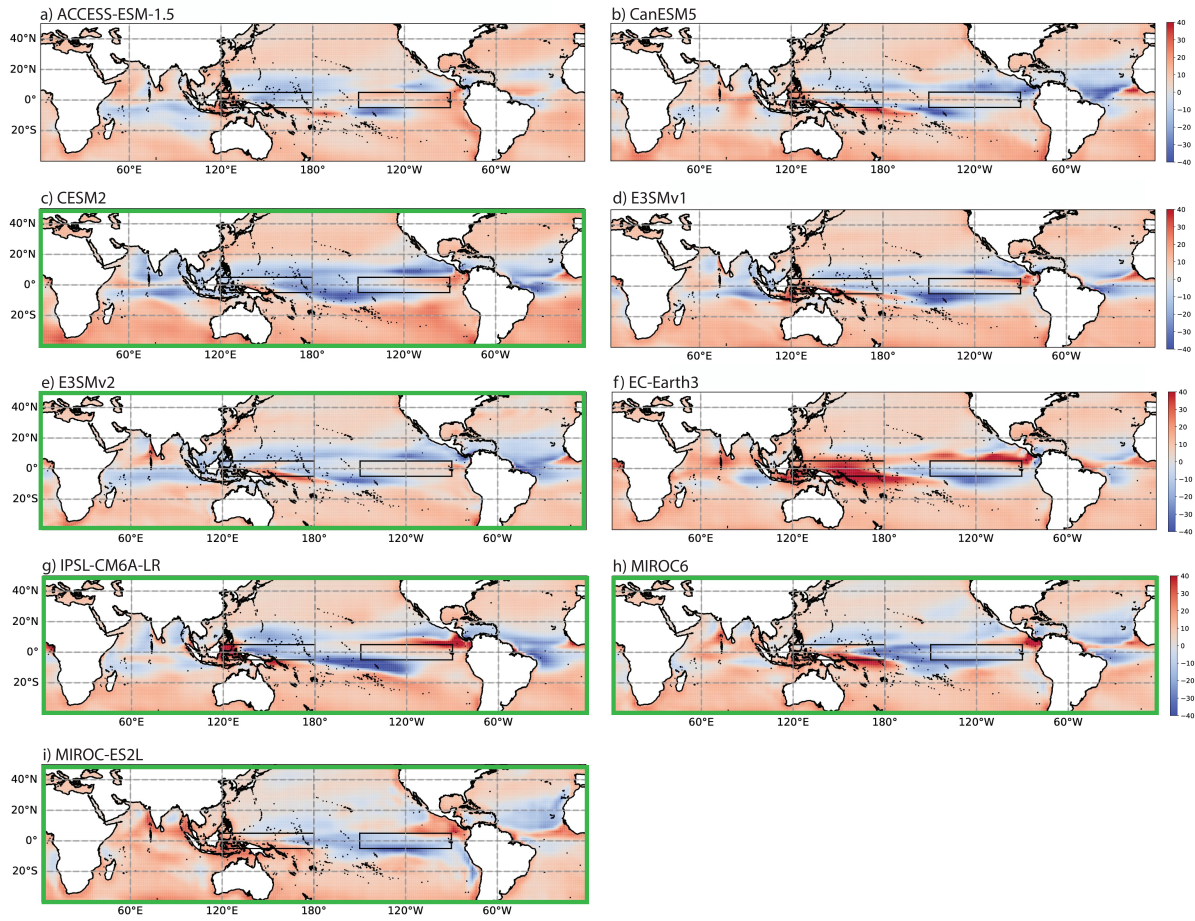


**Figure S3.** Differences in historical mean climate between models with high and low sensitivities of the equatorial Pacific SST gradient to climate change. a) Surface air temperature (C), for all calendar months. b) Precipitation (mm/day), for all calendar months. c), d) Same as a), b) for DJF. e), f) same as a), b) for JJA. "High" sensitivity models are those with ensemble-mean future - historical SST gradient differences above the 60th percentile of the set of all ensembles; "low" sensitivity models have SST gradient differences below the 40th percentile. Black stippling indicates locations where the differences between high and low sensitivity models are significant at the 95% level using a Wilcoxon rank-sum test. Historical values are calculated over the 1950-1999 period, as in the main text. SST gradients used to define percentile values are computed using all calendar months regardless of averaging season used for map fields.

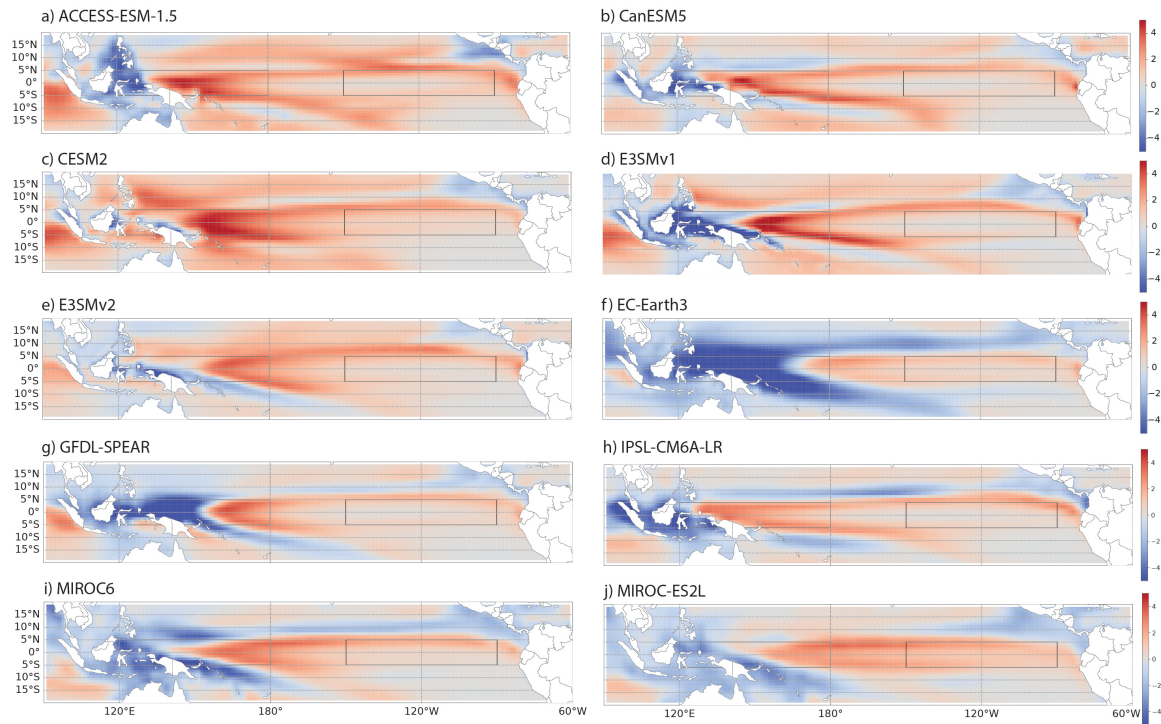


**Figure S4.** Historical mean values of a) precipitation and b) net surface shortwave radiation, averaged over all model ensembles.

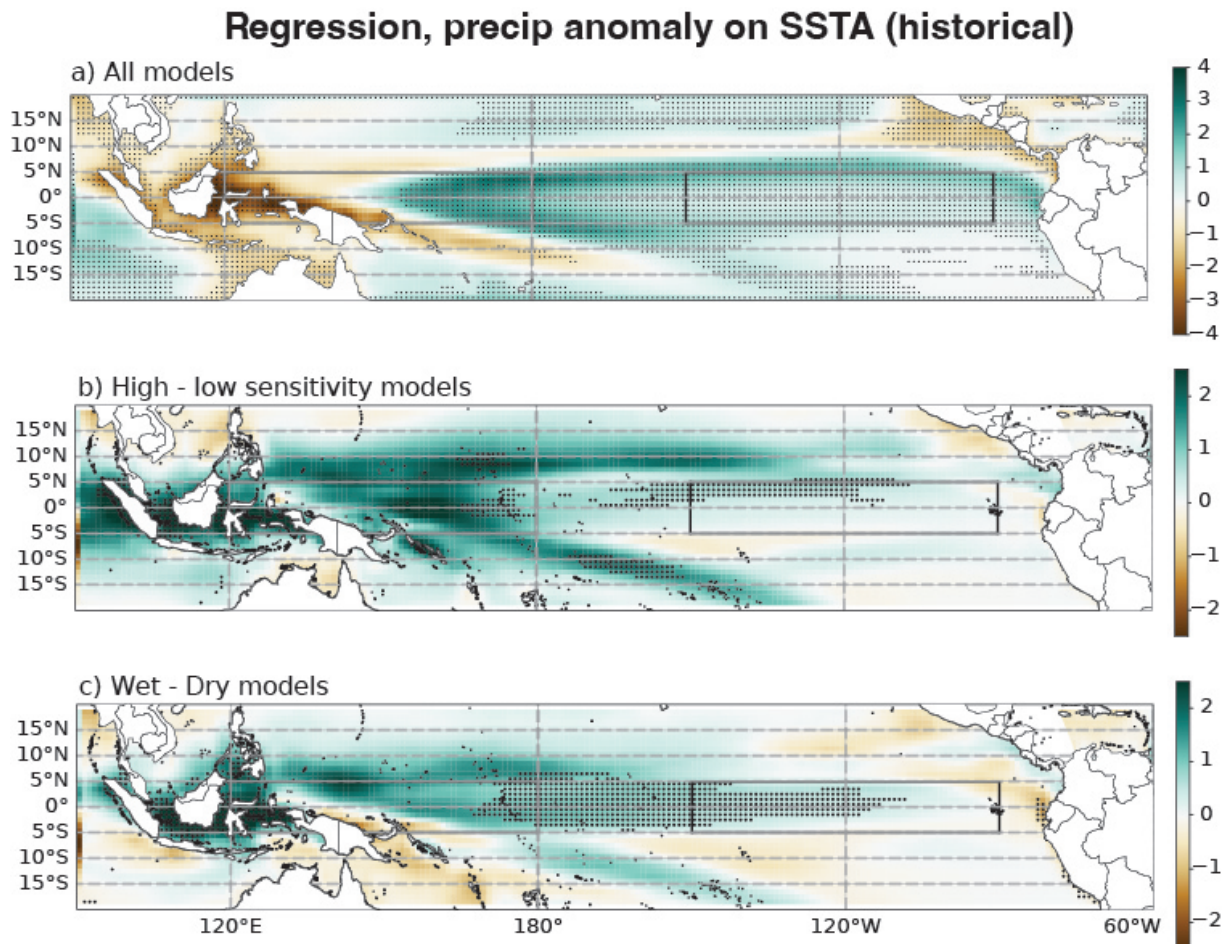




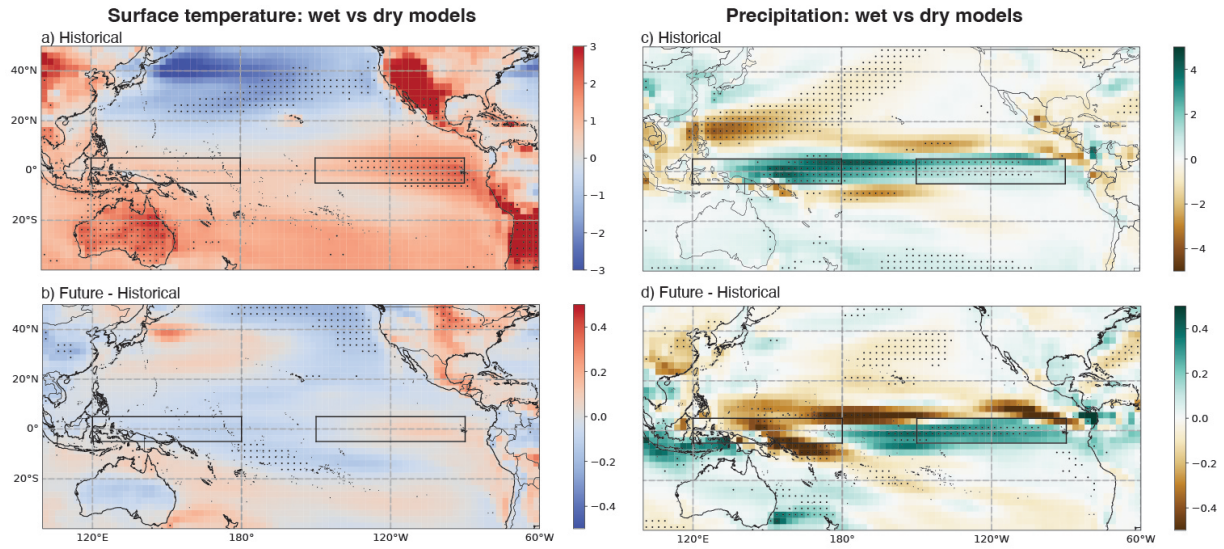
**Figure S5.** Regressions of net shortwave flux onto SSTA anomaly for individual ensembles used in the present analysis. Green bold panel outlines indicate models where historical climatological mean equatorial Pacific precipitation exceeds 4.5 mm/day (see Figure 5 in main text).



**Figure S6.** Sensitivity of precipitation to SSTA, diagnosed by gridpoint regression of precipitation anomaly on SSTA during the historical period for each individual model included in the present analysis.



**Figure S7.** Sensitivity of precipitation to SSTA, diagnosed by gridpoint regression of precipitation anomaly on SSTA during the historical period. a) Multi-ensemble mean for all models. b) Difference between high and low-sensitivity models. c) Difference between wet and dry models.





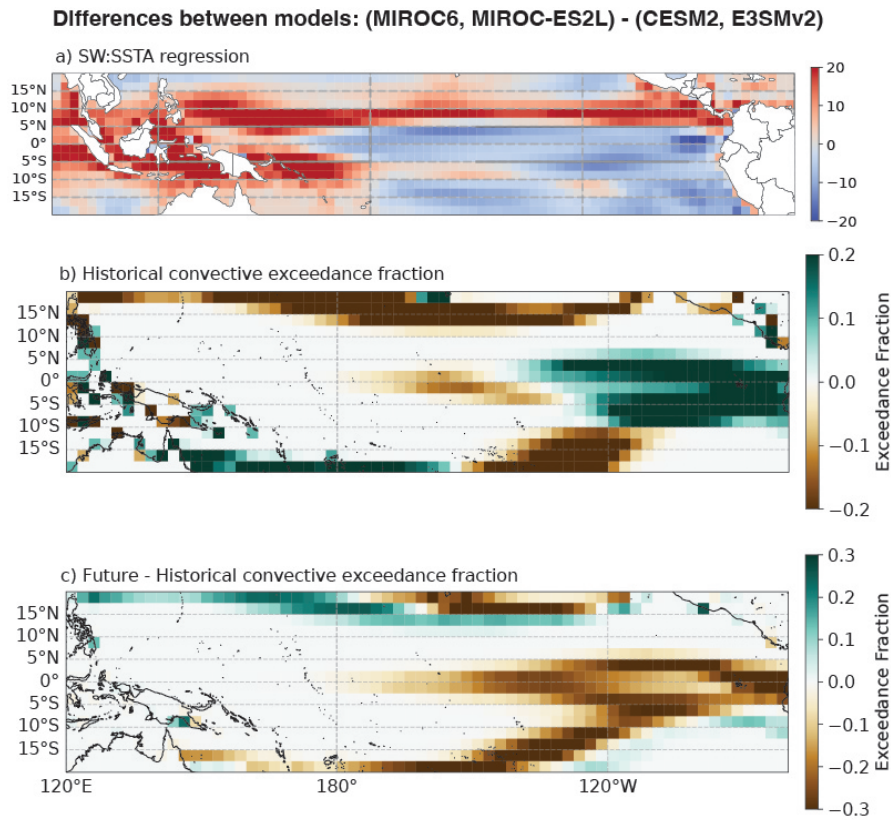


**Figure S9.** Behavior of shortwave feedback and convective exceedance fraction, differenced between the wettest two models (MIROC6 and MIROC-ES2L) and the next-wettest (CESM2 and E3SMv2). a) Gridpoint regression of net shortwave flux on SSTA, over the historical period. b) Convective exceedance fraction over the historical period. c) Convective exceedance fraction change, future - historical.

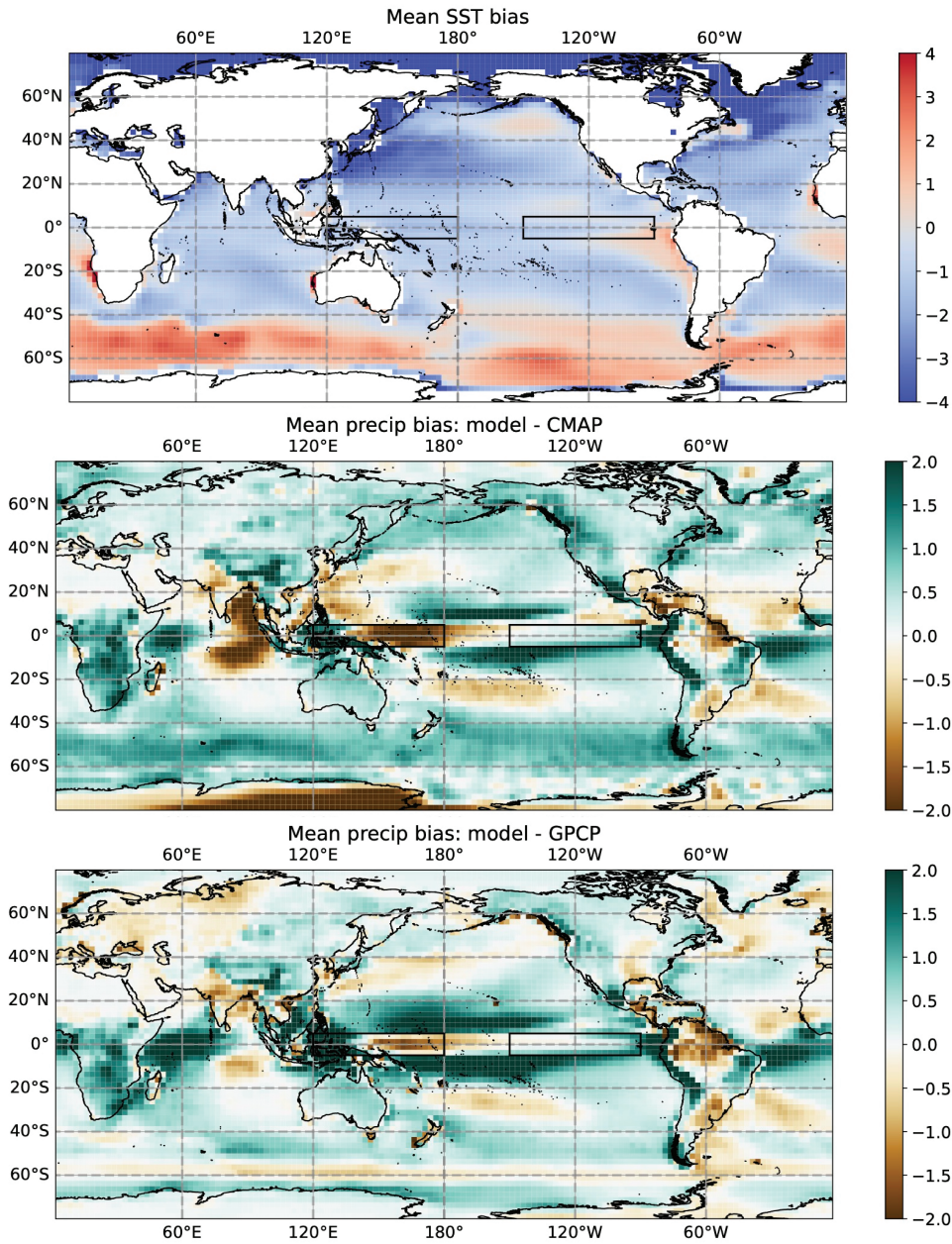


**Figure S10.** Multi-model mean historical bias in a) SST ( $^{\circ}\text{C}$ ), b) precipitation (CMAP), and c) precipitation (GPCP). Units for precipitation are mm/day. Bias maps are computed over the 1979-2024 period; ERSSTv5 is used for SST (little difference was seen between bias calculated with different SST datasets).

## References